ATTENUATION OF GROUND MOTION DURING THE 1995 GREAT HANSHIN EARTHQUAKE

by:
Gilbert L. MOLAS* and Fumio YAMAZAKI**

Introduction

Japan has been expecting an earthquake similar to the 1923 Great Kanto Earthquake for some years now. The residents of Kobe, however, did not expect it to occur so close to home. A magnitude 7.2 in the JMA scale occurred right under Kobe, which is one of the oldest and important economic hub of the region. It is the most destructive earthquake in Japan since the 1923 event (JMA, 1995; EERI, 1995).

There are several near source records from the Great Hanshin Earthquake (also called the Hyogo-ken Nanbu Earthquake and the Kobe Earthquake) on January 17, 1995. One of these is the record from the Japan Meteorological Agency (JMA) Kobe station. Although the epicentral distance is about 20 km, the activated fault runs very close to this station and the record can be considered as near-field. Since the earthquake occurred very close to a metropolitan area, several seismometers in the near-field were able to record the event. These near-field records are valuable because there are very few in Japan and they can help us understand the characteristics of near-field ground motion.

This study aims to evaluate the developed attenuation relations in light of the Great Hanshin Earthquake and to characterize the behavior of the near field records with respect to the far-field attenuation relations. Towards this end, it is necessary to summarize the data, methods, and results of the attenuation study.

Attenuation relations from records of the JMA stations

The acceleration time histories from the JMA stations under study were recorded by the new JMA-87 type seismometers. These digital seismometers have a flat sensitivity from 0.05 Hz to 10 Hz and can measure accelerations from 3×10^{-3} cm/s^2 to 980 cm/s^2 for periods from 1s to 10 min (JMA, 1991). Older SMAC-B2 seismometers have suppressed sensitivity in the high frequencies. Thus, correction procedures are needed for SMAC-B2 records (Kawashima et al., 1982, 1986). Records from JMA stations including events with depths of up to 200 km were used to develop attenuation relations for the peak ground acceleration (PGA) and peak ground velocity (PGV) for Japan (Molas and Yamazaki, 1995). Local-site effects (in terms of station coefficients) of 76 JMA stations were also determined. However, near source data are lacking and the attenuation relations are deemed valid only for far-field ground motion.

Table 1 shows the summary of the data used in the previous study. Although the number of records is large, the number of stations is fixed (i.e., 76 JMA stations using the JMA-87 seismometers). Figure 1 shows the epicenters of the earthquakes used in the previous study, which does not include the Great Hanshin Earthquake. It can be seen that many of the earthquakes are in eastern and northern Japan with few events in western and southern Japan. Thus, there are

* Post-doctoral Research Fellow, Institute of Industrial Science, University of Tokyo, 7-22-1 Roppongi, Minato-ku, Tokyo 106, Japan
** Associate Professor, ditto.

Table 1. Summary of data used for the attenuation study (Molas and Yamazaki, 1995)

No. of records	2,166
No. of recording stations	76
Date recorded	August 1, 1988 to December 31, 1993
Instrument	JMA-87 type accelerometers
Recording Institution	Japan Meteorological Agency (JMA)
Magnitude range	4.0 to 7.8 (JMA scale)
Minimum intensity (larger of two horizontal components)	PGA ≥ 1.0 cm/s
Depth range	0.1 km to 200 km

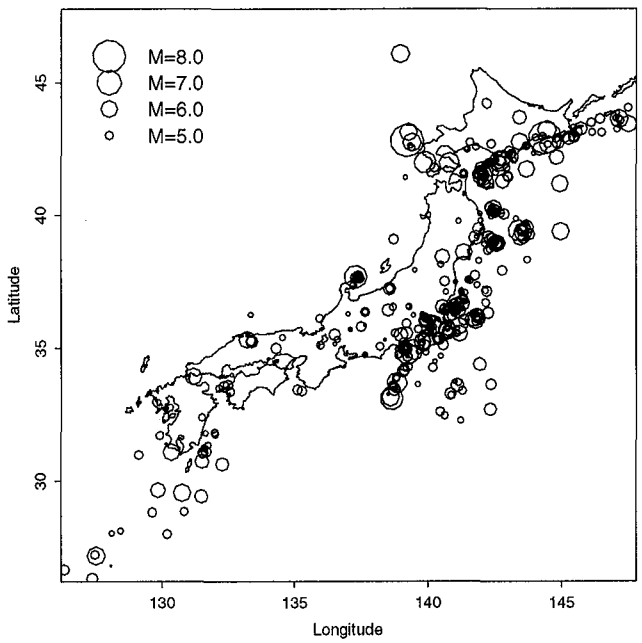

Figure 1. Epicenters of events used in the previous study (Molas and Yamazaki, 1995) to develop attenuation relations in Japan which includes deep events.

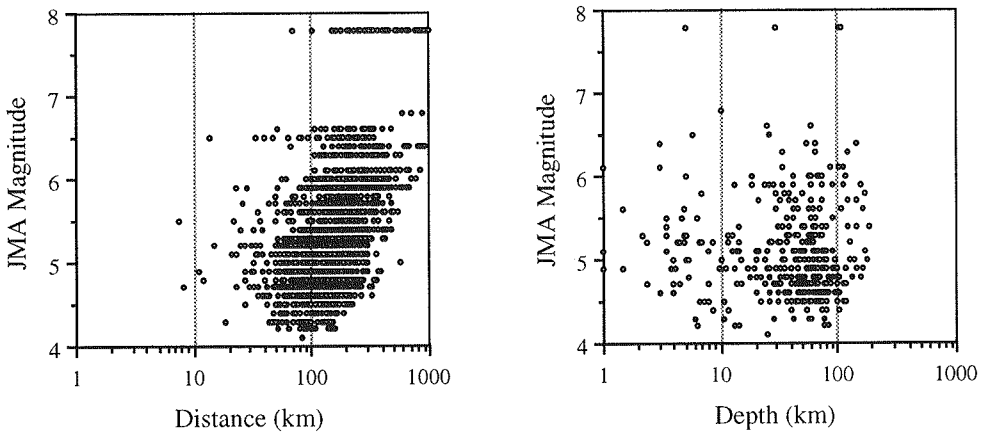

Figure 2. Distribution of the Magnitude vs. source-to-site distance, *r*, and Depth, *h*, used in the previous study

less records for the JMA stations in the west than in the east and north of Japan. Figure 2 shows the distribution of the data with respect to the magnitude, depth, and source-to-site distance. The plots show that there are no near-field records. Although the JMA Kushiro station is very close to the epicenter of the 1993 Kushiro-Oki earthquake (about 4 km), the source depth is about 100 km.

The PGA and PGV data were analyzed using a two-stage regression method (Joyner and Boore, 1981), which was found by Fukushima and Tanaka (1990) to be effective in eliminating the systematic error in regression resulting from the apparent correlation of the magnitude and slant distance. The effect of each recording station is considered in the regression instead of the commonly used soil-type classifications. However, the solution of the least squares regression for the first stage became singular, most likely because of the dummy variables for both the events and the recording stations. The regression is then solved by an iterative partial regression technique (Molas and Yamazaki, 1995). The resulting attenuation relations (PGA in cm/s^2 and PGV in cm/s) are:

$$\log_{10} PGA = 0.206 + 0.477M_J - \log_{10} r - 0.00144r + 0.00311h + c_i^a + 0.276P \qquad (1)$$

$$\log_{10} PGV = -1.769 + 0.628M_J - \log_{10} r - 0.00130r + 0.00222h + c_i^v + 0.257P \qquad (2)$$

where M_J is the JMA Magnitude, r is the shortest distance from the site to the fault plane, h is the depth of the point in the fault plane where r is measured, c_i is the station coefficient, and $P = 0$ for 50 percentile values or $P = 1$ for 84 percentile values. The resulting station coefficients for the 76 JMA stations in the study are given in Molas and Yamazaki (1995).

Recorded ground motion of the Great Hanshin Earthquake

Table 2 shows a summary of the ground motion recorded by JMA stations during the Great Hanshin Earthquake. Figure 3 shows the locations of the JMA stations. The triangles represent the JMA stations whose records are used in this study (see Table 2) while the squares represent the remaining JMA stations. Some JMA stations whose records were not used in this study are

closer to the epicenter (represented by x) than the stations whose records were used. This is most likely due to the low amplification rates (i.e., station coefficients) in the former. Although 45 stations recorded the acceleration time history of the earthquake, only the Kobe station can be considered as near-field. The JMA Kobe and Osaka stations have an epicentral distance of about 20 km and 50 km, respectively. As generally known, the use of epicentral or hypocentral distance in attenuation relations is not so good especially for events with long faults. The distance, r, in this study is defined as the shortest distance from the site to the fault surface. To measure this distance, the activated fault geometry must be estimated.

Kikuchi (1995) modelled the activated

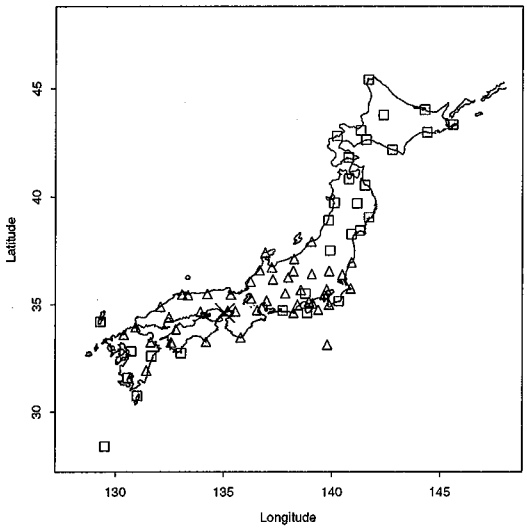

Figure 3. Location of JMA stations. Triangles show stations with records used in this study.

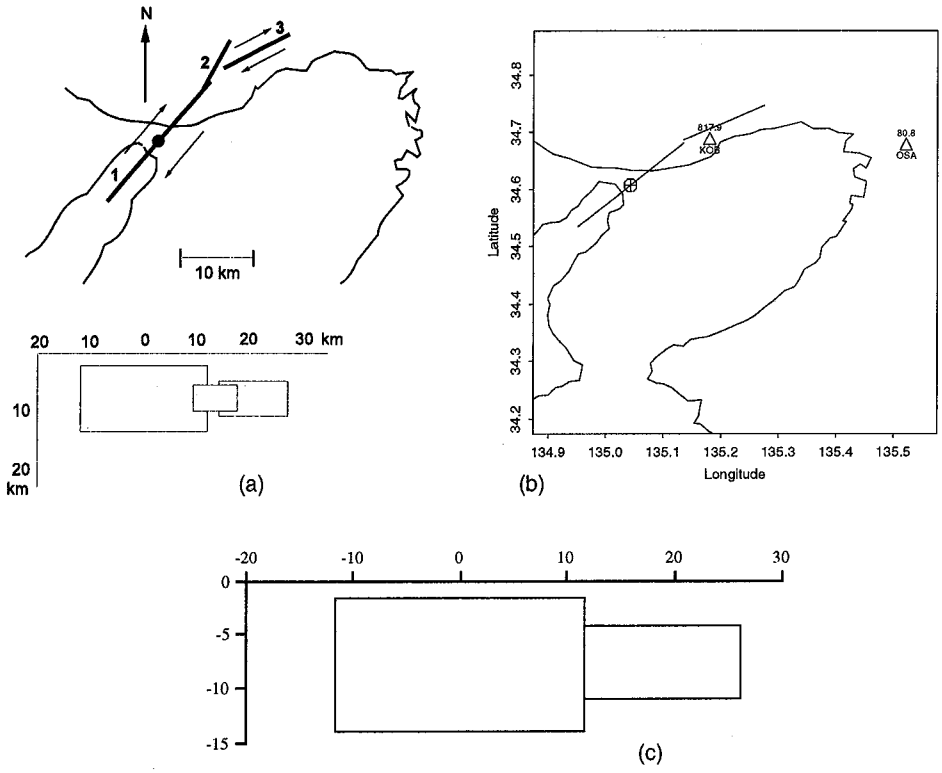

Figure 4. Fault model (a) proposed by Kikuchi (1995) and (b) modified fault model used in this study. The modified vertical section of the modified fault model is shown in (c).

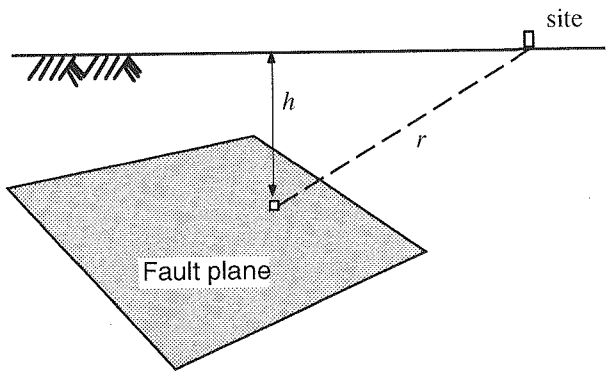

Figure 5. The distance term, r, and the depth term, h, are measured from the point in the fault plane where r is minimum. The fault plane is considered to be oriented in three-dimensional space.

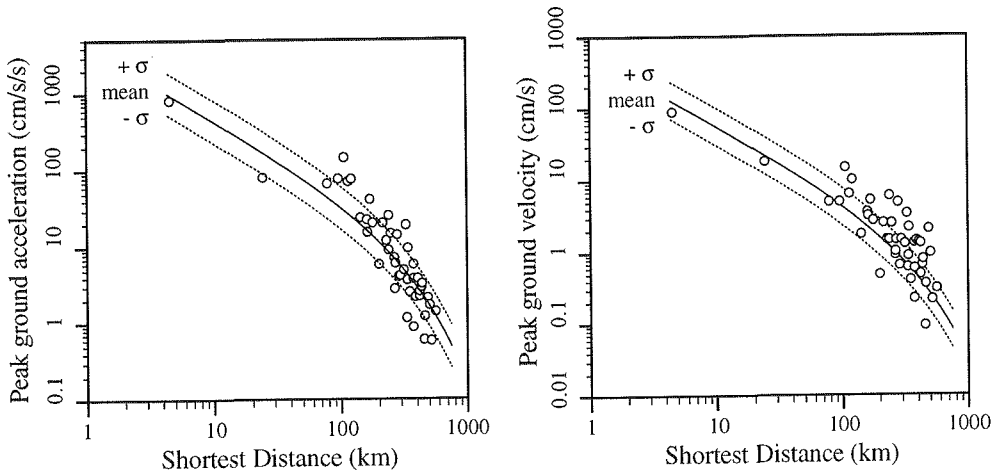

Figure 6. Recorded PGA (left) and PGV (right) of the Great Hanshin Earthquake from the JMA stations

fault as three strike-slip faults approximately extending from the southwest to northeast direction (Figure 4a). The activated faults have a dip angle of 90 degrees with varying dimensions and depth. To compute the shortest distance from the JMA stations, we used a simplified fault geometry based on Kikuchi. Since there are no stations very close to fault 2 and this fault is relatively smaller compared to the other two, it was disregarded in lieu of extending the north-eastern fault (fault 3) to be almost continuous with the south-western fault (fault 1). The adopted fault geometry is shown in Figure 4b. Although the activated fault model has three distinct faults, it is reasonable to assume that the recorded ground motions are superpositions of the ground motions from the three faults. Thus, we retained the JMA magnitude as 7.2. Table 2 lists the epicentral and shortest (slant) distances and the depth of the point in the fault that is closest to the JMA stations under consideration. The definition of distance, r, and depth, h, in this study is illustrated in Figure 5. In the case of the JMA Kobe station, although it is closer to the north-

Table 2. Summary of the Great Hanshin Earthquake data recorded by the JMA stations

	Station Code	Station Name	Epicentral Distance, D (km)	Shortest Distance, r (km)	Depth h (km)	Station Coefficient (PGA)	Station Coefficient (PGV)	Recorded PGA (cm/s/s)	Site-adjusted PGA	Recorded PGV (cm/s)	Site-adjusted PGV
1	AJI	Ajiro	377.61	350.56	4.3	0.2172	0.1050	2.54	1.54	0.41	0.32
2	CHO	Choshi	548.13	519.73	4.3	-0.1085	-0.0886	0.58	0.75	0.22	0.27
3	FKK	Fukuoka	440.75	434.69	1.7	0.2127	0.2586	2.95	1.81	0.66	0.37
4	FUK	Kawaguchiko	196.45	169.22	4.3	0.1244	0.1939	41.50	31.16	5.31	3.40
5	HIK	Hikone	136.29	106.36	4.3	0.1611	0.3232	146.89	101.36	15.02	7.14
6	HIR	Hiroshima	233.71	228.69	1.7	0.0620	0.1572	12.08	10.48	1.51	1.05
7	HJJ	Hachijojima	473.00	455.37	4.3	0.0721	0.0249	0.60	0.51	0.09	0.09
8	HMD	Hamada	269.69	266.34	1.7	-0.3126	-0.4815	2.81	5.77	1.02	3.10
9	IID	Iida	277.63	248.30	4.3	-0.0588	-0.1702	14.98	17.15	2.54	3.76
10	KAN	Kanazawa	266.20	239.03	4.3	0.1225	0.3122	25.55	19.27	6.06	2.95
11	KOB	Kobe	19.45	4.57	1.7	-0.1692	-0.0998	817.86	1207.48	89.50	112.63
12	KOF	Kofu	344.82	315.57	4.3	0.1324	0.1286	4.96	3.65	1.31	0.97
13	MAE	Maebashi	419.41	389.50	4.3	-0.2486	-0.2204	2.18	3.86	1.45	2.40
14	MAT	Matsushiro	362.75	332.90	4.3	-0.5085	-0.6683	1.15	3.72	0.62	2.88
15	MIS	Mishima	363.47	336.11	4.3	-0.0232	0.0073	3.66	3.86	0.89	0.87
16	MIT	Mito	533.90	504.40	4.3	0.3285	0.1874	1.71	0.80	0.98	0.63
17	MRT	Murotomisaki	168.49	159.88	1.7	-0.1056	-0.1369	22.66	28.90	3.64	4.98
18	MTM	Matsumoto	325.89	295.96	4.3	-0.3798	-0.3018	4.18	10.02	1.50	3.00
19	MTS	Matsue	199.93	199.71	1.7	0.1569	0.0925	5.91	4.12	0.49	0.39
20	MTY	Matsuyama	221.19	214.32	1.7	0.1224	0.1909	20.48	15.45	2.57	1.66
21	MYZ	Miyazaki	446.99	438.78	1.7	-0.2380	-0.0906	3.28	5.68	0.80	0.99
22	MZH	Maizuru	98.88	78.31	4.3	0.0156	0.0471	66.93	64.57	5.05	4.53
23	NAG	Nagoya	190.45	161.47	4.3	0.0242	0.0055	15.54	14.70	3.23	3.19
24	NII	Niigata	517.63	488.54	4.3	0.0053	0.1895	2.14	2.11	2.11	1.36
25	OIT	Oita	347.03	339.88	1.7	-0.0162	0.1177	9.61	9.97	2.21	1.69
26	OKA	Okayama	99.35	95.65	1.7	-0.0230	-0.1266	77.31	81.51	5.05	6.76
27	OMA	Omaezaki	294.44	269.56	4.3	-0.1800	-0.2351	6.09	9.21	1.48	2.54
28	ONA	Onahama	593.76	563.95	4.3	0.0369	0.0870	1.40	1.28	0.31	0.25
29	OSA	Osaka	48.75	24.27	4.3	-0.1143	0.0933	80.85	105.18	18.45	14.88
30	OSH	Oshima	400.09	374.32	4.3	0.1289	0.0726	0.87	0.65	0.22	0.19
31	SHJ	Shionomisaki	146.29	142.23	1.7	0.0720	-0.1429	24.05	20.38	1.79	2.49
32	SHN	Shimonoseki	381.57	375.93	1.7	0.0911	0.0925	5.88	4.77	0.59	0.48
33	SHZ	Shizuoka	314.21	287.25	4.3	-0.1922	-0.2515	4.08	6.35	0.65	1.17
34	TAT	Tateyama	447.06	420.42	4.3	0.0903	0.1813	2.23	1.81	0.49	0.32

Table 2. (*continued*)

	Station Code	Station Name	Epicentral Distance, Δ (km)	Shortest Distance, *r* (km)	Depth *h* (km)	Station Coefficient (PGA)	Station Coefficient (PGV)	Recorded PGA (cm/s/s)	Site-adjusted PGA	Recorded PGV (cm/s)	Site-adjusted PGV
35	TKD	Takada	404.62	375.29	4.3	0.2282	0.2523	3.79	2.24	1.36	0.76
36	TKY	Takayama	268.05	238.41	4.3	-0.2214	-0.3088	9.06	15.08	1.49	3.04
37	TOK	Tokyo	449.66	420.98	4.3	0.2249	0.1843	2.61	1.55	1.33	0.87
38	TOT	Tottori	120.45	120.73	4.3	0.1091	0.1914	76.74	59.69	10.17	6.55
39	TOY	Toyama	307.86	279.36	4.3	-0.1307	-0.1805	14.34	19.38	4.90	7.43
40	TSU	Tsu	140.25	114.35	4.3	0.0108	0.0450	70.99	69.25	6.48	5.84
41	UTS	Utsunomiya	491.38	461.57	4.3	0.0631	-0.0123	1.21	1.05	0.36	0.37
42	UWA	Uwajima	272.59	264.81	1.7	0.0000	0.0000	7.18	7.18	0.92	0.92
43	WAJ	Wajima	354.52	328.53	4.3	0.0564	0.1805	19.24	16.89	3.44	2.27
44	YOK	Yokohama	434.60	406.47	4.3	0.1028	0.2124	3.84	3.03	1.38	0.85
45	YON	Yonago	177.27	177.57	1.7	0.1046	0.0704	20.58	16.17	2.77	2.36

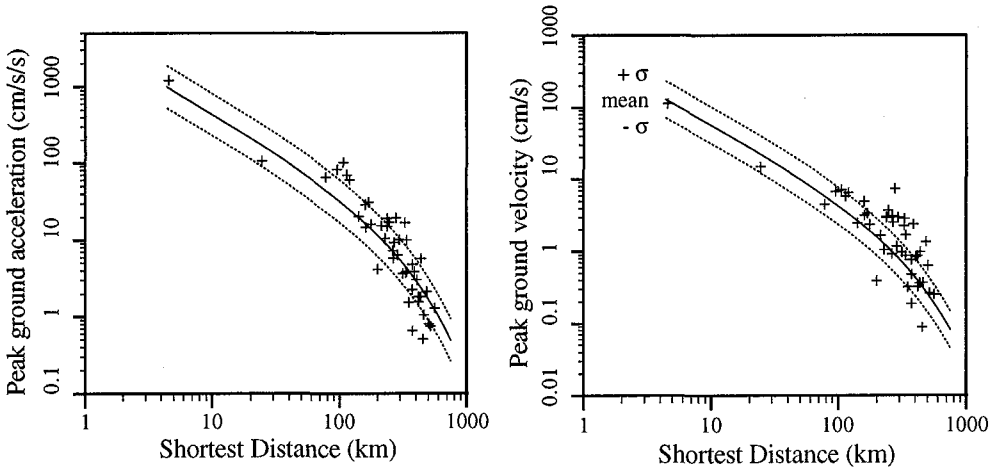

Figure 7. Site-adjusted PGA (left) and PGV (right) of the Great Hanshin Earthquake from the JMA stations

eastern fault horizontally, the shortest slant distance is from the south-western fault whose extent is closer to the surface. Figure 6 shows the recorded PGA and PGV with respect to the closest distance. The fitting of the data with respect to the predicted peak ground motion looks very good even for near-field data if we simply use the shortest distance to the fault. However, by taking into account the local site effect of each recording station, the fitting can still be improved (Molas and Yamazaki, 1995). Figure 7 shows the PGA and PGV adjusted for the local site effect. It can be seen that the fitting is improved. Although the predictive equations were developed from far-field data, the near-field data from JMA Kobe station has a good fit with Equations 1 and 2.

The importance of the definition of distance in the near-field has been recognized by many researchers (e.g., Boore and Joyner, 1982; Singh et al., 1989; Ohno et al., 1993) Ohno et al. proposed a redefinition of distance taking into consideration the fault geometry. After this redefinition, they showed that the attenuation characteristics of near-field records assume those of far-field records. As shown in Figures 6 and 7, by defining the distance, r, as the shortest distance from the site to the fault plane, the near-field record fit well with the attenuation relation. Since this is only one data point, however, it is premature to draw conclusions.

Effect of the Great Hanshin Earthquake data on the attenuation equations

There are a lot of good near-field records for the Hanshin earthquake, which are rather rare in Japan. It is therefore interesting to investigate how the near-field data affects the attenuation relations derived from far-field data. Unfortunately, at this moment, only the JMA records are possible to integrate into the original data set. Using the original data selection criteria, 41 of 45 records are selected. However, the record at Uwajima is further excluded because there are no other record from this JMA station. The resulting data set therefore has 2,206 records from 388 events and 76 stations.

The results of the iterative partial regression for PGA and PGV are

$$\log_{10} PGA = 0.184 + 0.482M_J - \log_{10} r - 0.00149r + 0.00315h + c_i^a + 0.278P \qquad (3)$$

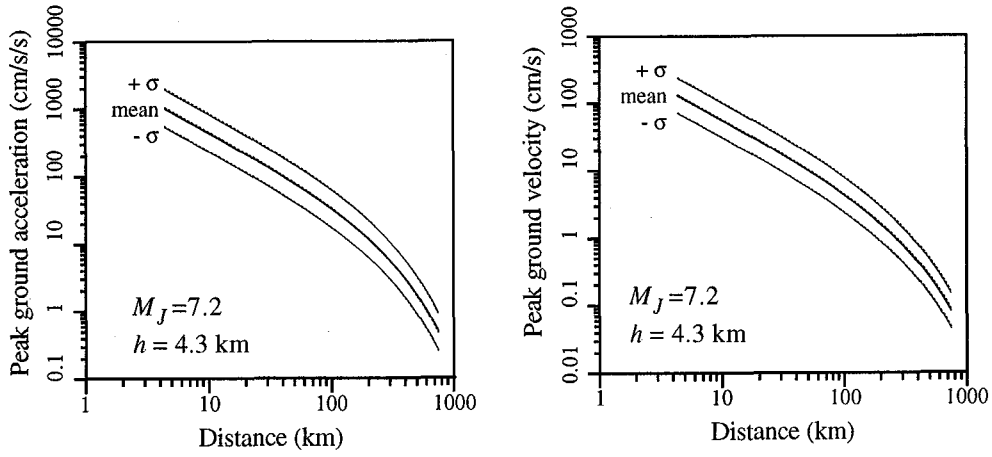

Figure 8. Attenuation curves for Equation 1 (solid lines) and computed attenuation relation considering the data of the Great Hanshin Earthquake (dotted lines)

$$\log_{10} PGV = -1.781 + 0.631M_J - \log_{10} r - 0.00127r + 0.00211h + c_i^a + 0.259P \qquad (4)$$

where the variables are defined as in Equation 1. There is little difference compared to the original attenuation relation. Figure 8 shows the predicted attenuation curves of the original and new attenuation relations for the Hanshin earthquake ($M = 7.2$, $h = 4.3$ km) and the confidence limits based on one standard deviation. The attenuation curves are very close to each other. This is to be expected since the influence of the new data is small given the large number of data used in the original data set. The relatively good fit of the Great Hanshin Earthquake data to the original predictive curves means that the improvement of the regression fit by including the new data will be small. In the case of the near-field record in the JMA Kobe station, the predicted PGA from the original attenuation equation is close to the recorded and adjusted PGA. Thus, the effect on the regression is also very small.

Other near-field records

Several organizations collected near-field data from the Great Hanshin Earthquake. Near-field data are few in Japan because many events occur offshore and may be very deep. The non-JMA near-field data used in this study were collected from various publications which reported on the Great Hanshin Earthquake. We selected data that were recorded on free-field conditions and excluded those that were recorded by the SMAC-B2 instrument. Table 3 summarizes the non-JMA data used in this study. Most of these data have a shortest distance, r, less than 100 km. The locations of the data close to the fault are given in Figure 9. This figure also shows the relative PGA and PGV of the near-field records and clearly shows that the largest peak ground motions occur along the activated fault surface. Figure 10 shows the plot of these data with the JMA data with respect to the shortest distance. The JMA data in this figure are the recorded PGA and PGV without correcting for the station effect. Since the station coefficients of the non-JMA stations are unknown, corrections are not possible. The figure shows that non-JMA recorded PGAs and

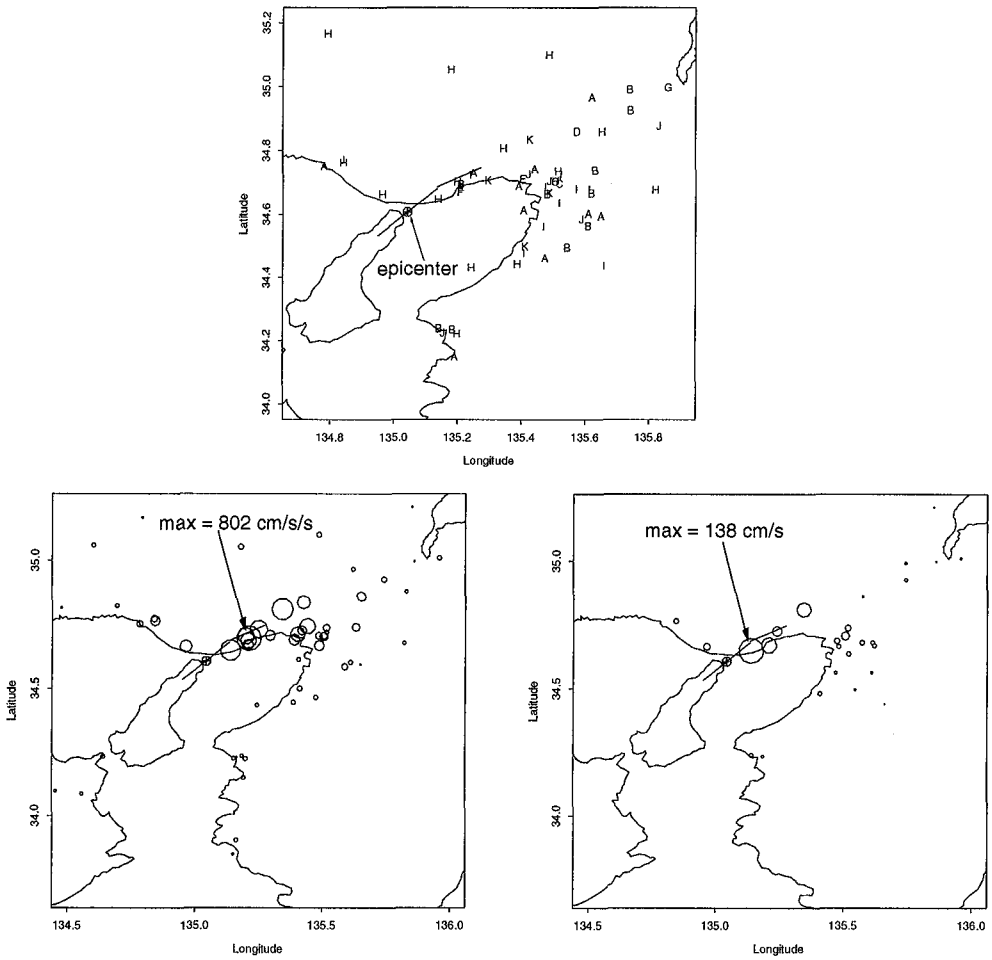

Figure 9. Location of non-JMA near-field data (top) and the distribution of the peak ground acceleration (bottom left) and peak ground velocity (bottom right) in the near-field.

PGVs have a good fit with Equation 1 and 2, respectively. Figure 10 also shows the confidence limits of one standard deviation. It must be noted that these standard deviations are based on the fact that the station effects are explicitly determined and therefore does not contain the station-to-station component of the variance. For non-corrected data, the correct confidence limits should include the station-to-station component, therefore the confidence limits should be a bit wider than those in Figure 10.

In our previous study, we did not consider the effect of near-source data in the attenuation relations because there are no near-field records from the JMA stations that we studied. The predicted attenuation curves in Figure 10 show a rather straight line as the distance approaches zero. It has been shown theoretically and statistically that there exist a limit on the ground motion very near the fault rupture due to the limit on the energy that the earth's material can release due

Table 3. Summary of non-JMA data used in this study

Station Code	Station Location	Latitude (deg)	Longitude (deg)	Shortest Distance, r (km)	Depth, h (km)	PGA (cm/s/s)	PGV (cm/s)
Kansai Electric Power Co.							
A-1	Miyatsu Energy Res. Inst.	35.554	135.256	89.98	4.30	69.9	
A-2	Yamazaki Experiment Center	35.060	134.603	64.12	4.30	131.3	
A-3	West Kyoto Substation	34.967	135.622	40.33	4.30	129.3	
A-4	Shin-Kobe Substation	34.731	135.250	4.34	4.30	584.3	
A-5	Takasago Power Station	34.753	134.783	28.24	1.70	198.0	
A-6	Ako Power Station	34.735	134.379	56.96	1.70	103.6	
A-7	General Technical Res. Inst.	34.743	135.442	15.91	4.30	506.6	
A-8	Amagasaki-3 Power Station	34.690	135.391	13.13	4.30	353.6	
A-9	Nanko Power Station	34.614	135.408	19.71	4.30	125.8	
A-10	Yao Substation	34.603	135.611	35.02	4.30	148.0	
A-11	Shinki Substation	34.594	135.650	38.60	4.30	46.1	
A-12	Minami-Osaka Substation	34.464	135.475	36.74	4.30	146.0	
A-13	Kainanko Substation	34.150	135.192	48.16	1.70	128.2	
A-14	Gobo Power Station	33.850	135.150	78.33	1.70	74.0	
A-15	Yusaki Substation	33.672	135.350	102.76	1.70	18.5	
Osaka Gas							
B-1	East Supply Department	34.668	135.619	32.99	4.30		23.0
B-2	Fujiidera	34.564	135.609	37.04	4.30		12.7
B-3	Kyoto Supply Station	34.992	135.741	50.79	4.30		13.5
B-4	Soyama Supply Station	34.496	135.544	37.48	4.30		11.0
B-5	Matsue Supply Station	34.240	135.141	37.16	1.70		21.8
B-6	Iwasaki Supply Station	34.665	135.481	21.39	4.30		24.0
B-7	Fukiai Supply Station	34.695	135.211	4.91	4.30	802.0	
B-8	Shijo-Nawate Supply Station	34.739	135.632	33.00	4.30	256.5	
B-9	Fushimi Supply Station	34.926	135.743	47.46	4.30	178.0	17.6
B-10	Nakanoshima Supply Station	34.236	135.185	39.62	1.70	106.5	15.1
Takenaka Corporation							
C-1	Osaka, Kita-ward	34.703	135.505	22.07	4.30	267.4	
C-2	Osaka, Kita-ward	34.698	135.519	23.47	4.30	50.3	
Research Center for Earthquake Prediction , Disaster Prevention Research Institute, Kyoto University							
D-1	Abusan	34.860	135.574	30.41	4.3		10.4
D-2	Asai	35.477	136.324	125.55	4.30		2.5
D-3	Oya	35.322	134.666	82.81	4.30		3.9
D-4	Kume	35.089	133.849	118.13	1.70		3.4
D-5	Wachi	35.282	135.401	60.87	4.30		31.7
Ministry of Transport, Ports and Harbors Research Institute							
E-1	Kobe Port	34.686	135.209	5.33	4.30	502.0	
E-2	Amagazaki Port	34.712	135.404	13.20	4.30	471.7	
Kobe City Governent							
F-1	Port Island	34.670	135.208	6.38	4.30	341.2	87.3
Shiga Prefectural Government							
G-1	Ashibiya	35.209	135.851	73.70	4.30	37.0	6.2
G-2	Torahime	35.416	136.265	117.09	4.30	70.0	6.9
G-3	Mizuguchi	34.968	136.170	85.55	4.30	43.0	4.1
G-4	Osakaya	34.998	135.861	60.59	4.30	45.0	6.6
G-5	Kusatsu	35.011	135.958	69.14	4.30	145.0	11.6
G-6	Imazu	35.403	136.035	100.77	4.30	47.0	4.2

Table 3. (*continued*)

Station Code	Station Location	Latitude (deg)	Longitude (deg)	Shortest Distance, r (km)	Depth, h (km)	PGA (cm/s/s)	PGV (cm/s)
JR Railway Technical Research Institute							
H-1	Nishi-Akashi	34.6640	134.964	9.73	1.70	397.0	39.2
H-2	Takatori	34.6490	135.139	3.24	1.70	666.0	138.0
H-3	Shin-Kobe	34.7040	135.200	4.42	4.30	530.0	
H-4	Kakogawa	34.7640	134.843	25.34	1.70	313.0	27.9
H-5	Himeji	34.8225	134.694	39.51	1.70	125.0	
H-6	Takarazuka	34.8090	135.344	10.33	4.30	694.0	80.0
H-7	Higashi-Kishiwada	34.4450	135.388	34.84	4.30	144.0	
H-8	Wakayama	34.2240	135.199	41.39	1.70	143.0	
H-9	Shin-Osaka Station	34.7060	135.506	22.11	4.30	228.0	45.3
H-10	Shin-Osaka Substation	34.7370	135.516	22.55	4.30	229.0	34.4
H-11	Aioi	34.8150	134.476	53.59	1.70	62.0	
H-12	Sasayamaguchi	35.0530	135.180	35.40	4.30	177.0	
H-13	Ikuno	35.1666	134.793	62.09	4.30	53.0	
H-14	Shin-Takatsuki	34.8590	135.654	37.13	4.30	297.0	
H-15	Sonobe	35.1000	135.487	44.04	4.30	163.0	
H-16	Iri	34.7510	134.208	72.23	1.70	97.0	
H-17	Nara	34.6770	135.821	50.81	4.30	112.0	
H-18	Fukuchiyama	35.2930	135.121	62.52	4.30	107.0	
H-19	Gobo	33.9040	135.162	72.79	1.70	132.0	
H-20	Kansai Int'l Airport	34.4334	135.244	26.77	1.70	117.0	
The Committee of Earthquake Observation and Research in the Kansai Area (CEORKA)							
I-1	Kobe University	34.725	135.240	4.31	4.30		55.1
I-2	Fukushima	34.687	135.474	19.08	4.30		31.0
I-3	Morikouchi	34.680	135.572	27.76	4.30		27.1
I-4	Yae	34.680	135.612	31.29	4.30		21.8
I-5	Chihaya-Asakasa	34.4390	135.659	49.36	4.30		5.2
I-6	Sakai	34.564	135.469	26.41	4.30		15.9
I-7	Tadaoka	34.480	135.408	31.30	4.30		24.4
I-8	Abeno	34.636	135.519	25.02	4.30		24.9
Ministry of Construction							
J-1	Kakogawa Dike	34.7725	134.8386	27.30	1.70	211.0	
J-2	Amagasaki Bridge	34.7264	135.4206	13.54	4.30	294.0	
J-3	Kinokawa Embankment	34.2256	135.1533	38.09	1.70	129.0	
J-4	Yodogawa Embankment (Oyodo)	34.7056	135.4861	19.60	4.30	224.0	
J-5	Yodogawa Dike	34.7194	135.5167	22.08	4.30	138.0	
J-6	Yamatogawa Embankment	34.5861	135.5881	33.18	4.30	199.0	
J-7	Yoshinogawa Embankment (Tokushima)	34.0864	134.5575	61.36	1.70	110.0	
J-8	Yoshinogawa Embankment (Ishii)	34.0983	134.4547	66.50	1.70	90.0	
J-9	Anogase Dam	34.8781	135.8306	52.69	4.30	107.0	
J-10	Naruto	34.2340	134.6410	43.92	1.70	136.00	
Hanshin Expressway Corporation							
K-1	Higashi-Kobe Bridge	34.7065	135.296	6.52	4.30	326.0	
K-2	Inagawa	34.8360	135.427	17.65	4.30	421.0	
K-3	Kanjyo Yotsubashi	34.6670	135.488	21.91	4.30	324.0	
K-4	Matsunohama	34.5000	135.413	30.54	4.30	169.0	

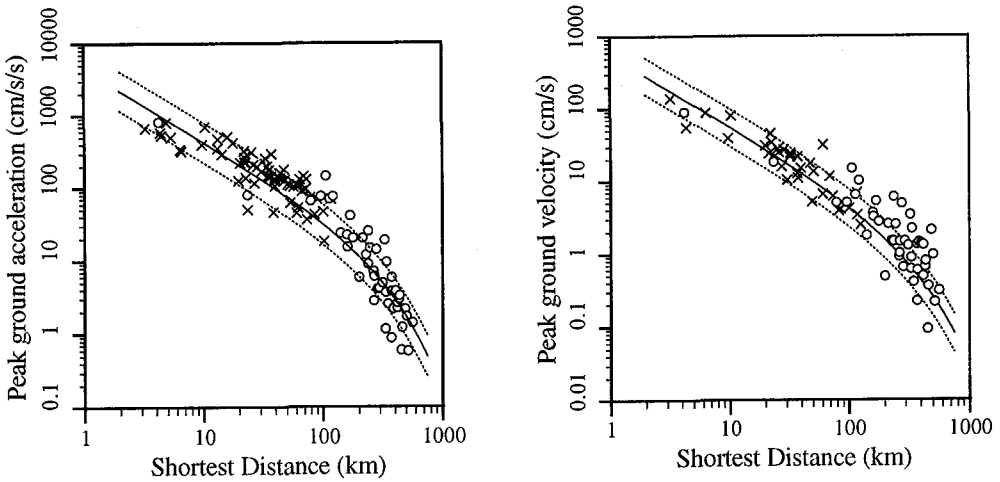

Figure 10. Plot of recorded PGA (left) and PGV(right) for the JMA stations (circles) and other free-field (non-JMA) recording stations (x's). The solid line shows the predicted mean PGA and PGV using Equation 1 and 2, respectively while the dotted lines give the one-standard deviation confidence limits. The standard deviation is based on the regression which considers the local-site effect of the JMA stations. The confidence limits for data uncorrected for local site effect should include the station-to-station component of the variance. This component, however, was not estimated in our previous study.

to its finite strength. Several attenuation relations which consider the near-field assume a magnitude-dependent distance parameter which limits the predicted peak ground motion in the near-field. This is usually achieved by making the distance parameter approach a finite value instead of zero at sites close to the fault. From Figure 10, it is apparent that the data with distances less than 10 km will have a much better fit if the attenuation curves become flat at distances less than 10 km, especially the data with a distance less than 5 km. The depth of the north-eastern fault (4.3 km) is highly influential in this range.

However, this observation is based on one event only and we need more data to be able to precisely predict ground motion in the near-field. The results of the previous study show that the local-site effect is very important in attenuation relations. The use of simple soil-type classification does not provide adequate information on the amplification of a single site and this can lead to large errors, especially if used in hazard and risk analyses which are based on single sites. It is still unclear how the site effects of the non-JMA stations used in this study will affect the attenuation relation in the near-field. However, based on previous results, considering the local-site effect decreases the scatter of the data from the best fit line.

Modified attenuation relation in the near-field

In the light of the preceding observations, it is possible to use the near-field data of the Great Hanshin Earthquake to introduce modifications to Equations (1) and (2) for use in the near-field. However, since the data available is limited to one earthquake only, the modifications should be used with careful consideration of this fact.

The attenuation characteristics in the near-field has been studied by Campbell (1981) using data from the US supplemented by worldwide data. Based on the theoretical considerations, Campbell used the attenuation relation of the form:

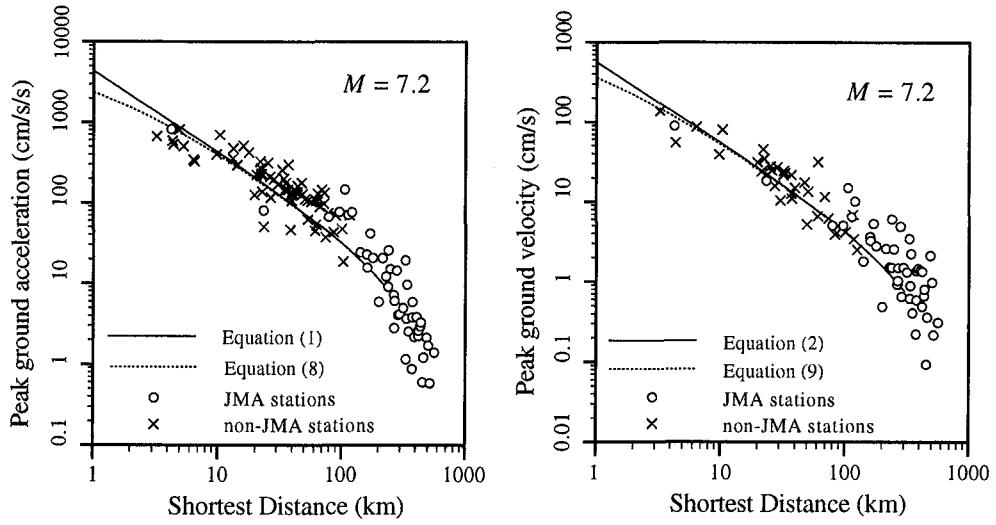

Figure 11. Modified attenuation curves at the near-field region for PGA (left) and PGV (right)

$$PGA = a\exp(bM)[R + C(M)]^{-d} \tag{5}$$

where

$$C(M) = c_1 \exp(c_2 M) \tag{6}$$

This form is supported by geological and seismological studies. The term c_1 is related to the distance saturation while c_2 is related to the magnitude saturation. Studies have shown that the PGA near the fault rupture is magnitude independent. To satisfy this condition, the following constraint is imposed:

$$c_2 = b/d \tag{7}$$

In the case of Japan, Fukushima and Tanaka (1990) supplemented the Japanese data with near-field data of Campbell (1981). They constrained their regression model such that the peak ground acceleration near the fault rupture is magnitude-independent. Kamiyama et al. (1994), used a semi-empirical model to obtain a magnitude-independent peak ground acceleration and magnitude-dependent peak ground velocity and displacement near the fault rupture.

Since the near-field data for this study is limited to one earthquake, it is not possible to verify if the data supports magnitude-independence. However, we believe that there are enough arguments to support magnitude independence of peak ground acceleration near the fault rupture. Therefore, in the near-field, Equation (1) and (2) are modified to reflect distance and magnitude saturation as

$$\log_{10} PGA = 0.206 + 0.477M_J - \log_{10}\left(r + C^a(M)\right) - 0.00144r + 0.00311h + c_i^a + 0.278P \tag{8}$$

$$\log_{10} PGV = -1.769 + 0.628M_J - \log_{10}\left(r + C^v(M)\right) - 0.00130r + 0.00222h + c_i^v + 0.259P \tag{9}$$

where

$$C(M) = d_1 \exp(d_2 M) \tag{10}$$

Similar to Fukushima and Tanaka (1990), we applied the distance adjustment only for the geometric spreading term. This is because in the near-field, anelastic attenuation is negligible relative to geometric spreading. If total magnitude-independence of the peak ground acceleration is assumed, d_2 is set equal to the magnitude scaling parameter (i.e., $d_2 = 0.477$). However, since the near-source data used is from a single event, we limit our determination of the near-field saturation to that of $C^a(M)$ and $C^v(M)$. These values are assumed to be constant until more near-field data are acquired. To estimate $C(M)$, we perform a non-linear least square analysis of the Great Hanshin Earthquake data (JMA and non-JMA). This is done by the GOLDEN search algorithm (Press, et al., 1992) to iteratively find $C(M)$ such that the sum of squares of the errors are minimized. The parameter $C(M)$ was found to be 0.82 km for PGA and 0.55 km for PGV. The $C(M)$'s determined from the least-squares analysis seem small which suggests that the distance saturation is not so influential in this data set. If the magnitude of the Great Hanshin earthquake is used as a reference, we can compare the distance saturation parameters from other studies. Campbell (1981) determined a $C(M)$ for PGA of 7 km for unconstrained magnitude independence and 21.3 km for a magnitude independent PGA at the near-field (assuming a Richter Magnitude of 6.8). Fukushima and Tanaka assumed magnitude independence of PGA and determined a $C(M)$ of 28.1 km. Kamiyama et al. (1994) also assumed magnitude independence of PGA and determined a $C(M)$ of 38.3 km. Although Kamiyama et al. did assumed magnitude dependence for the PGV and the PGD, they used the same $C(M)$ as in the PGA.

The resulting attenuation curves are shown in Figure 11. In this figure, the curves were drawn assuming that $h = 0$. Since h is small, the contribution of the depth term to the predicted peak ground motion is negligible. It can be seen from Figure 11 that the results of the minimization analyses are not so different from the original attenuation relations except for the very near-field. This is to be expected since the data used in the analysis have a good fit to the original attenuation curve and that there are relatively few data points in the very-near-field region. More near-field data are needed to improve the prediction of near-field peak ground motion.

Conclusions

The earthquake ground motion data recorded during the Great Hanshin Earthquake are examined and compared with the results of an attenuation study based on earthquakes before the Great Hanshin Earthquake. Since the previous study is based on data from JMA stations recorded by the new JMA-87 type seismometers, the records from these stations are compared with the predicted attenuation curves. It is found that the recorded data have a relatively good fit. The fit is improved if the recorded data are corrected for local-site effects determined from the previous study. Since the attenuation relations were derived from far-field data, it is encouraging that the near-field data also fit the predicted attenuation. However, the data are still inadequate for a more definite conclusion.

Since there are several near-field data for the Great Hanshin Earthquake, the attenuation is also compared to the predictive equations. It is found that the near-field non-JMA data also have good fit with the attenuation relations based on far-field data. It is apparent that the fit will improve if the attenuation relations constrain the predicted PGAs and PGVs at the near-field to a finite-value. The attenuation relations developed from far-field data was modified by redefining the distance parameter for the geometric spreading term. Although magnitude independence of the PGA in the near-field is desirable, it is not possible to determine such

characteristics at this time. The distance parameter was assumed to be a constant and determined such that the sum of squares of the errors are minimized. The resulting attenuation curves have improved fit in the near-field but the saturation effect is not so influential to the Great Hanshin Earthquake data set.

Acknowledgment

We are grateful to the Japan Meteorological Agency (JMA) for providing us the acceleration time histories of the JMA stations, to the Committee of Earthquake Observation and Research in the Kansai Area (CEORKA) and other institutions for providing the near-source data.

References

Architectural Institute of Japan (AIJ). Preliminary Reconnaissance Report of the 1995 Hyogoken-Nanbu Earthquake, 1995.

Boore, D. M. and W. B. Joyner (1982). The empirical prediction of ground motion, *Bull. Seism. Soc. Am.* **72**, no. 6, S43-S60.

Campbell, K. W. (1981). Near-source attenuation of peak horizontal acceleration, *Bull. Seism. Soc. Am.* **71**, no. 6, 2039-2070.

Earthquake Engineering Research Institute (EERI). The Hyogo-ken Nanbu Earthquake - Preliminary Reconnaissance Report, 1995.

Fukushima, Y. and T. Tanaka (1990). A new attenuation relation for peak horizontal acceleration of strong ground motion in Japan, *Bull. Seism. Soc. Am.* **80**, no. 4, 757-783.

Japan Meteorological Agency (JMA) (1991). Earthquake Observer Guide. (in Japanese)

Joyner, W. B. and D. M. Boore (1981). Peak horizontal acceleration and velocity from strong-motion records including records from the 1979 Imperial Valley, California, earthquake, *Bull. Seism. Soc. Am.* **71**, 2011-2038.

Kamiyama, M., M.J. O'Rourke, and R. Flores-Berrones (1994). A semi-empirical model of strong ground motion peaks with appropriate comparisons to the 1989 Loma Prieta, the 1985 Michoacan and the 1971 San Fernando Earthquakes, *Japan Soc. Civil Eng, Jour. Struct. Mech Earthquake Eng* **10**, no. 4, 29-39.

Kawashima, K., K. Aizawa, and K. Takahashi (1986). Attenuation of peak ground acceleration, velocity and displacement based on multiple regression analysis of Japanese strong motion records, *Earthquake Eng. Struct. Dyn.* **14**, 199-215.

Kawashima K., Y. Takagi, and K. Aizawa (1982). Accuracy of digitization of strong-motion records obtained by SMAC-accelerograph, *Proc. Japan Soc. Civil Engineers, no. 323*, 647-75.

Kikuchi, M. (1995). Rapid seismic source information from the far field waveform, *Proc. Safety Engineering Symposium*, pp. 127-130. (In Japanese)

Molas, G. L. and F. Yamazaki (1995). Attenuation of earthquake ground motion in Japan including deep focus events, *Bull. Seism. Soc. Am.* **85**, no. 5 (to appear)

Nakamura, Y., K. Hidaka, J. Saita, and S. Sato (1995). JR Earthquake Information No. 23b - Strong accelerations and damage of the 1995 Hyogo-ken Nanbu Earthquake. Railway Technical Research Institute. (In Japanese)

Ohno, S., T. Ohta, T. Ikeura, and M. Takemura (1993). Revision of attenuation formula considering the effect of fault size to evaluate strong motion spectra in near field, *Techtonophysics* **218**, 69-81.

Press, W. H., S. A. Teukolsky, W. T. Vetterling, B. P. Flannery (1992). Numerical Recipes in C, 2nd Ed. Cambridge University Press.

Singh, S. K., M. Ordaz, J.G. Anderson, M. Rodriguez, R. Quass, E. Mena, M. Ottaviani, and D. Almora (1989). Analysis of near-source strong motion recordings along the Mexican subduction zone, *Bull. Seism. Soc. Am.* **79**, 1697-1717.